Manifold Learning for Image-Based Gating of Intravascular Ultrasound(IVUS) Pullback Sequences

Gozde Gul Isguder[1], Gozde Unal[1], Martin Groher[2], Nassir Navab[2],
Ali Kemal Kalkan[3], Muzaffer Degertekin[3], Holger Hetterich[4],
and Johannes Rieber[4]

[1] Sabanci University,
[2] Technical University Of Munich,
[3] Yeditepe University Hospital,
[4] Ludwig Maximilian University Hospital
{isguder,gozdeunal}@sabanciuniv.edu, {groher,navab}@in.tum.de,
{akalkan,mdegertekin}@yeditepe.edu.tr,
{Holger.Hetterich,Johannes.Rieber}@med.uni-muenchen.de

Abstract. Intravascular Ultrasound(IVUS) is an imaging technology which provides cross-sectional images of internal coronary vessel structures. The IVUS frames are acquired by pulling the catheter back with a motor running at a constant speed. However, during the pullback, some artifacts occur due to the beating heart. These artifacts cause inaccurate measurements for total vessel and lumen volume and limitation for further processing. Elimination of these artifacts are possible with an ECG (electrocardiogram) signal, which determines the time interval corresponding to a particular phase of the cardiac cycle. However, using ECG signal requires a special gating unit, which causes loss of important information about the vessel, and furthermore, ECG gating function may not be available in all clinical systems. To address this problem, we propose an image-based gating technique based on manifold learning. Quantitative tests are performed on 3 different patients, 6 different pullbacks and 24 different vessel cuts. In order to validate our method, the results of our method are compared to those of ECG-Gating method.

Keywords: Manifold Learning, Classification, IVUS, Image-based gating, ECG gating.

1 Introduction

Intravascular Ultrasound is a unique invasive catheter-based imaging technology, which yields a high resolution, real-time cross-sectional view of the blood vessels from the inside-out. The cross-sectional images are acquired by pulling the catheter back with a motor running at a previously defined constant speed, and this whole process is referred as a pullback. Since IVUS modality provides a very detailed information about the internal vessel structures, it is a unique

tool for the diagnostics of coronary artery diseases(CAD) and plaque characterization. For diagnosis and assessment of the disease, accurate measurements of the total vessel and the lumen volume in the suspicious lesion areas are crucial. However, quality of the IVUS evaluations, and accuracy of the measurements deteriorate due to artifacts caused by heart movement during a pullback[1]. The most obvious artifact is the back and forth movement of the catheter in the vessel longitudinal direction due to the periodical change in the blood flow while the heart muscles are contracting and expanding. In [2], the authors observe that the IVUS transducers within coronary vessels have a longitudinal movement of average 1.50±0.80 mm during each cardiac cycle. As the transducer moves back and forth, it passes through the same locations of the vessel multiple times; thus it oversamples the vessel. This means gaining unnecessary information which leads to computational inefficiency for further processing. Furthermore, due to the movement, the longitudinal cut of the vessel has a saw-toothed appearance(see Fig. 5 first row) which makes the segmentation of the vessel even harder. Another artifact caused by the cardiac cycle is the change of the vessel morphology due to the varying blood pressure during the cycle. The change in the morphology leads to the variations in the lumen area observed at different cardiac phases(systole,diastole). In [1,2], it is stated that measured lumen and vessel volumes in non-gated image sets are significantly larger than normal and the choice of the suitable phase is still a question. A way to account for the problems above is introducing an electrocardiogram (ECG) signal, which is capable of giving information about the heart's current physical status. By utilising the ECG signal, heart and IVUS transducer are synchronized so as to capture the frames only near the predetermined fraction of the RR-interval[1]. However online-ECG gating requires an ECG unit, which may not be always available to the physician. Furthermore, in the older systems that used ECG triggering, ECG gating increased the image acquisition time, and in the new systems, the acquisition time is not affected but some important information about the vessel is lost.

In this paper, we introduce a robust image-based gating method based on manifold learning. By designing this method, our overall aim is to retain only the necessary information about the vessel, (the frames at a particular fraction of the RR-interval), which will be good enough to provide accurate lumen volume measurements and vessel length; at the same time will avoid loss of important plaque information in the lesion areas.

2 Related Work

In [3], a method for classification of the IVUS frames as end-diastolic and not end-diastolic is presented. As preprocessing, important image characteristics such as edges are enhanced, different feature vectors based on spatial and frequency characteristics of the images are defined, and finally a nearest neighbor search based on the Euclidean distance between the feature vectors is used to classify the frames.

In [4], a method to retrieve the cardiac phase by examining the features in a circular region of interest, namely Average Intensity(AI) and Absolute Intensity Difference between the subsequent frames, was discussed.

In [5,6], an image-based gating algorithm is proposed where a Dissimilarity Matrix based on the Normalized Cross Correlation (NCC) is built between each 2-tuples of the pullback; then the matrix is filtered with an X-shaped inverted Gaussian kernel, which highlights the frames with high similarity. Finally an algorithm to find the highest local maxima along the path on the diagonals, that represents the optimal gating frames, is introduced.

In [7], the authors use a similar technique to [5], by building the dissimilarity matrix D based on the image descriptors which are defined based on Gabor patches. A 1D signal is extracted from D, which defines the similarities between the frames and finally a local minimum search over the 1D signal is performed to obtain the best frames.

3 Our Contribution

In all the methods discussed above, even if different techniques were used, the overall objective is to be able to construct a 1D signal similar to R-waves by using the information(features) that is embedded in the images. In this paper, we propose directly projecting our high dimensional data, to a low-dimensional manifold and thus treating each image frame as a low-D signal in the low-D manifold.

A variety of dimensionality reduction techniques have been proposed in the literature, ever since emergence of complex and high-dimensional input data. The most commonly used linear dimensionality reduction techniques such as Principal Component Analysis(PCA) and Multi-dimensional scaling(MDS) are efficient and simple, however are not able to detect nonlinear structures that exist almost in all true datasets. The human cardiac system is nonstationary,dynamic and nonlinear; hence, linear analyses may not account for all aspects of cardiac performance[8,9].

Manifold learning is an effective, geometrically motivated, nonlinear dimensionality reduction technique, which is used to solve a variety of vision problems such as segmentation, registration, tracking and object recognition. The technique was validated to be successful, particularly if the input has smooth appearance variation or smooth deformation[12]. As explained in Section 1, cardiac cycle's first effect, slowly varying longitudinal movement of the catheter, results in a smooth appearance variation. Furthermore, the slight vessel morphology change during the cycle results in a smooth deformation in the input images.

In addition, in the lesion areas where the cross-sectional view of the vessel can change faster, using global distance metrics would fail because the lesion areas would be detected as outliers. However manifold learning preserves locality, which makes it much less sensitive to noise and outliers.

With the motivation provided above, our contribution in this paper, is to adopt and apply the manifold learning framework to our problem of image-based gating of IVUS pullbacks as explained in the next section.

4 Method

Isomap [10], local linear embedding [11], and Laplacian eigenmaps [12] are three different techniques for manifold learning. In this paper we will use Laplacian eigenmaps technique, which is very simple and efficient since it solves only one sparse eigenvalue problem. We construct our problem as follows:

Given a set of k points $x_1, ..., x_k$ in $\mathbb{R}^d$, where k is the number of frames x_i in the pullback and d is the dimension of the image; find another set of k points $y_1, ..., y_k$ in $\mathbb{R}^m$, where $m \ll d$. We assume that $x_1, ..., x_k \in \mathcal{M}$, where $\mathcal{M}$ is a manifold embedded in $\mathbb{R}^d$.

An important issue is the choice of the dimension of the $\mathcal{M}$, denoted by m. We need one dimension to account for the smooth appearance variation caused by
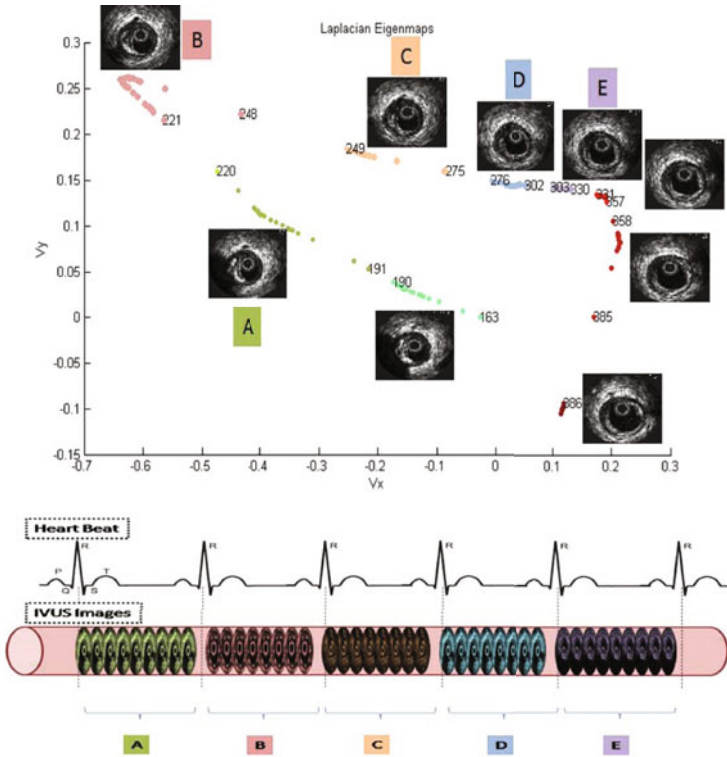

Fig. 1. An illustration of Manifold idea. Each frame is shown with a dot on the calculated low-D manifold(here m=2), where A,B,C,D,E are the clusters of frames that belong to different cardiac cycles.

the first artifact, and another dimension to account for the smooth deformation caused by the second artifact (see Section 3). Thereby, we choose $m \geq 2$. We heuristically choose $m = 3$. In another words we choose to represent each image frame with a 3D vector.

4.1 Laplacian Eigenmaps

Laplacian eigenmaps[12] is an approach that incorporates the neighborhood information of the input to build a weighted graph. After building the graph, a low-D representation of the input that optimally preserves local neighborhood information, is computed by using the Laplacian of the graph. It is worth noting that, since the approach is geometrically motivated, the resulting mapping will be a discrete approximation of a continuous map from the high dimensional space to the low-D manifold.

The first step is to construct the graph with representative k nodes for each x_i and edges between the nodes x_i and x_j , if the nodes are close enough. The relationship of being close can be defined as an ϵ neighborhood $||x_i - x_j|| < \epsilon$, where $||.||$ denotes the Euclidean norm. The disadvantage of this choice is the parameter setting. Another option is using n nearest neighbors, where one can put an edge between the nodes x_i and x_j if j is one of the n nearest neighbors of i. If we define the approximate number of frames in each cardiac cycle as n_{cycle}, the parameter n should satisfy $n \geq n_{cycle}$.

Another important issue is defining a similarity measure for the nodes x_i and x_j. In our weighting function we used Sum of Squared Distances(SSD), but different measures such as Sum of Absolute Difference(SAD) or Normalized Cross Correlation (NCC) can also be used.

The second step is to weight the edges in the graph by the appropriate weights. Weight function is inspired from the heat equation given by

$$W_{ij} = exp^{-||x_i - x_j||^2/2\sigma^2} \tag{1}$$

where σ^2 is the variance. $W = [W_{ij}]; ij \in [1, .., k]$, forms the weight matrix.

As a final step, a diagonal weight matrix D is constructed by summing up the coloumns of W, and Laplacian $L = D - W$ is then calculated. The eigenvectors corresponding to the smallest eigenvalues (excluding zero) of the Laplacian matrix gives the desired mapping. We refer to [12] for further details on the Laplacian eigenmap method.

4.2 Clustering

In general there are about ≈ 90 cardiac cycles in each pullback(see Table 2). However, to illustrate the idea of manifold learning, a desired mapping for 9 sequential cardiac cycles is given in Fig. 1. In Fig. 1, the low-D manifold gives a very nice intuition of the clusters that belongs to the same cardiac cycle. We observed that the largest distance between the eigenvectors V_i and V_{i+1} occurs if V_i is the last frame that belongs to the nth cardiac cycle and V_{i+1} is the starting

frame of the $(n + 1)^{st}$ cardiac cycle. The distance signal $d = ||V_{i+1} - V_i||$ is constructed. Since the method preserves the local-distances, the global structure is more visible after normalization of d. In Fig. 2, constructed d function for 400 frames is shown for illustration, where green boxes indicate the local maxima points in d function.

In order to find the local maxima points of the distance function d, we utilise a morphological eroding operation. Let $min_{cluster}$ be the minimum number of frames in a cluster, then a structuring element of size $min_{cluster}$ is constructed and distance signal is eroded with the structuring element. If the current point is a local maximum around the structuring element, then eroding operation will not change its value, thus we check for the points that has not changed after the eroding operation. This very simple but efficient technique finds the local maxima points. In some cases, where the frames of the sequential cardiac cycles are too similar, e.g branching areas, the distance function may not have any local maxima. In other cases, where the frames of one cardiac cycle are too different (e.g lesion areas where vessel changes rapidly), the distance function may have more than one local maxima. In those cases, we refine the results of the local maxima and check the number of frames between each possible consecutive maximum. If the difference between the two consecutive possible maximum points is bigger than $2n_{cycle}$, we look for another local maximum between them, and if the difference is smaller than $n_{cycle}/2$ we eliminate the possible maximum. After the post-processing step, local maxima of the distance function d, hence the gated(stable) image frames are obtained, and the IVUS gating algorithm is completed.

5 Experiments and Results

We applied our automatic image-based gating algorithm on 3 different patients and 6 different pullbacks. All the pullbacks were acquired in-vivo in the coronary
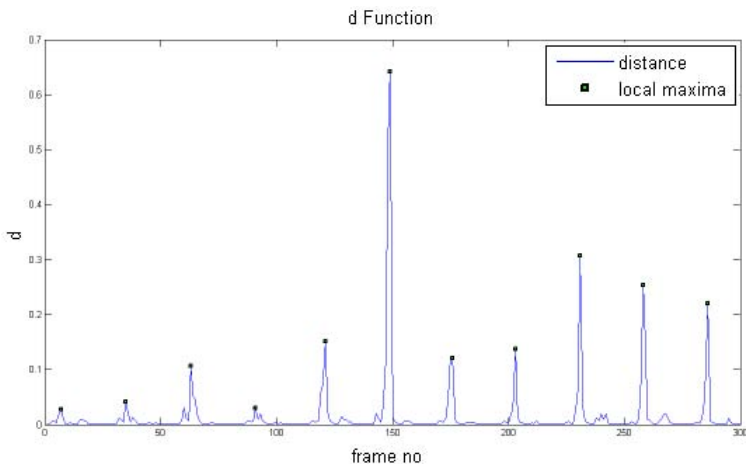

Fig. 2. Normalized Distance Function

Table 1. Lumen Area Differences Error Analysis, where pt_{id} is the patient id, pb_{id} is the pullback id, angle is the viewing angle for constructing a longitudinal cut and LAD Error is the lumen area difference error

pt_{id}	1				2				2				3				3				3			
pb_{id}	1				1				2				3				1				2			
Angle	10	50	130	150	10	50	130	150	10	50	130	150	10	50	130	150	10	50	130	150	10	50	130	150
LAD Error	0.02	0.04	0.02	0.02	0	0.05	0.1	0.1	0.07	0.03	0.07	0.09	0.02	0	0.03	0	0.03	0.01	0	0.02	0.08	0.1	0.01	0.01
Mean Error	0.02				0.06				0.06				0.01				0.01				0.05			

arteries of the patients of our clinical partners with 40 MHz IVUS catheter. The frame rate was 30 Hz and the motorized pullback speed was 0.5 mm/s.

In our method, we used n_{cycle} to represent the number of frames per cardiac cycle. n_{cycle} is defined as $f_{Rate}/1.2Hz$, where 1.2 Hz is the average heart beat rate of human species and f_{Rate} is the frame rate of the pullback. Similarly $min_{cluster}$ is used to represent the minimum number of frames in a cardiac cycle. $min_{cluster}$ can be equated to $f_{Rate}/(1.2Hz+2\sigma)$, where σ is the variance of the heart beat rate. The variance of the heartbeat may be high in the patients with irregular heart beats. Choosing a large σ would guarantee to find the local maxima points in d function for those patients. However, the latter may lead to too many possible local maxima points. In our experiments, we choose a small $\sigma = 0.1Hz$.

In order to validate our results, we compared the number of gated frames obtained by our algorithm and by ECG gating algorithm. In Table 2, the number of gated frames from the two methods show agreement. As stated in Section 3, the accurate measurements of lumen is crucial for coronary artery diseases' diagnostics. For that reason, we compared the lumen areas calculated from our gated pullbacks and ecg gated pullbacks. The lumen areas were drawn by the expert cardiologists in our team. For more accurate results, we compared the
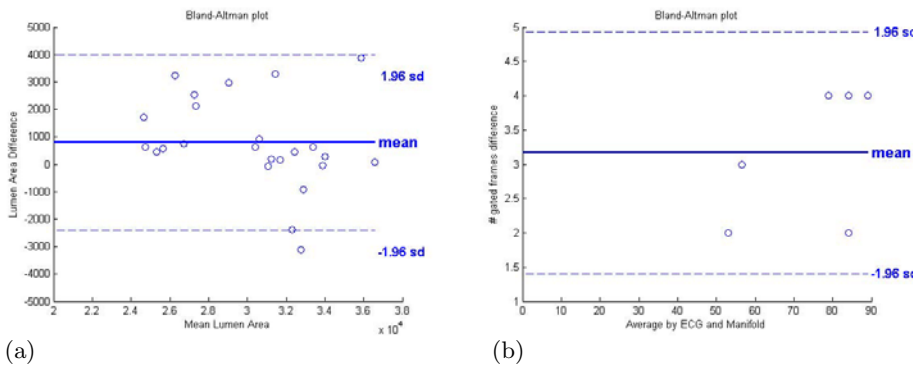

(a)   (b)

Fig. 3. (a)Bland-Altmann Analysis of Lumen Areas drawn by the medical experts on ecg gated pullback and image-based gated pullback: 790 ± 40.79 pix. (b) Bland-Altmann Analysis of gated frame normalized count calculated by ecg gating and image-based gating: 3.1667 ± 0.937.

Table 2. Comparison of the frame counts chosen by ecg gating algorithm and our image based gating algorithm. pt_{id} is the patient id, pb_{id} is the pullback id, $\#ecg$ represents the number of frames chosen by ecg, $\#alg$ shows the frame count selected by our algorithm and length[mm] is the actual length of the vessel.

pt_{id}	pb_{id}	#total	#ecg	#alg	length[mm]
1	1	2328	81	77	38.80
2	1	1627	54	52	27.12
2	2	1800	58	55	30.00
3	1	2388	85	83	39.80
3	2	2379	86	82	39.65
3	3	2358	91	82	39.30

lumen areas in the longitudinal views of the vessel from 4 different angles for each pullback. In Fig 4, an illustration of vessel longitudinal cuts at different angles is given. Difference(LAD) error in Table 1 is calculated as the ratio of the absolute difference of the areas found by the two methods, with the ecg-gated pullback area used as the ground truth: $LAD_{error} = |LA_{ecg} - LA_{alg}|/LA_{ecg}$, where LA_{ecg} is the lumen area in the ecg gated pullback and LA_{alg} in the image based gated pullback. An LAD error rate of 0.04 ± 0.03 is obtained. In addition, a Bland-Altmann analysis on the lumen areas (Fig. 3.a), revealed that more than 95% of the measurements were in agreement between the two methods. In Fig. 3.b, a plot for the Bland-Altmann analysis based on the number of gated frames calculated by both methods is given. To account for the different vessel lengths among our dataset, we considered the normalized counts, computed as #gated / #total. Longitudinal IVUS views shown in Fig 5, demonstrate similar qualitative outcome for our manifold-learning based IVUS gating method, and the ECG-gated method, which is also verified by the expert cardiologist in the team.
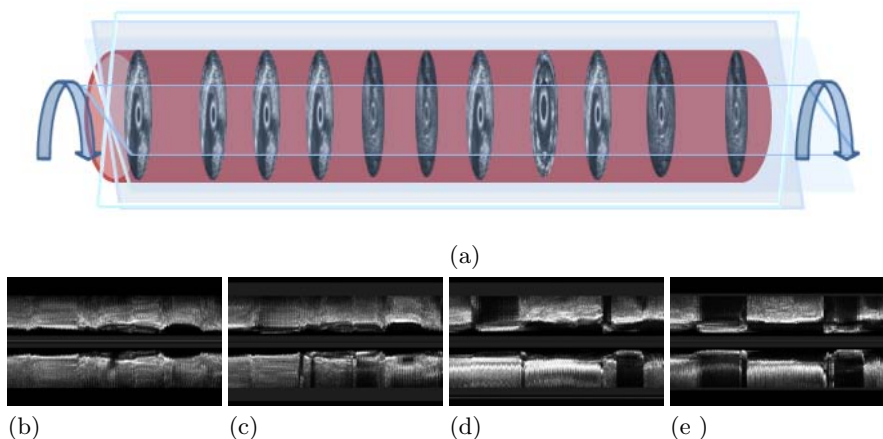

(a)

(b)　　　　　(c)　　　　　(d)　　　　　(e)

Fig. 4. (a)An illustration of longitudinal cuts(LC) at different angles (b) LC from $10°$ (c) LC from $50°$ (d) LC from $130°$ (e) LC from $150°$.
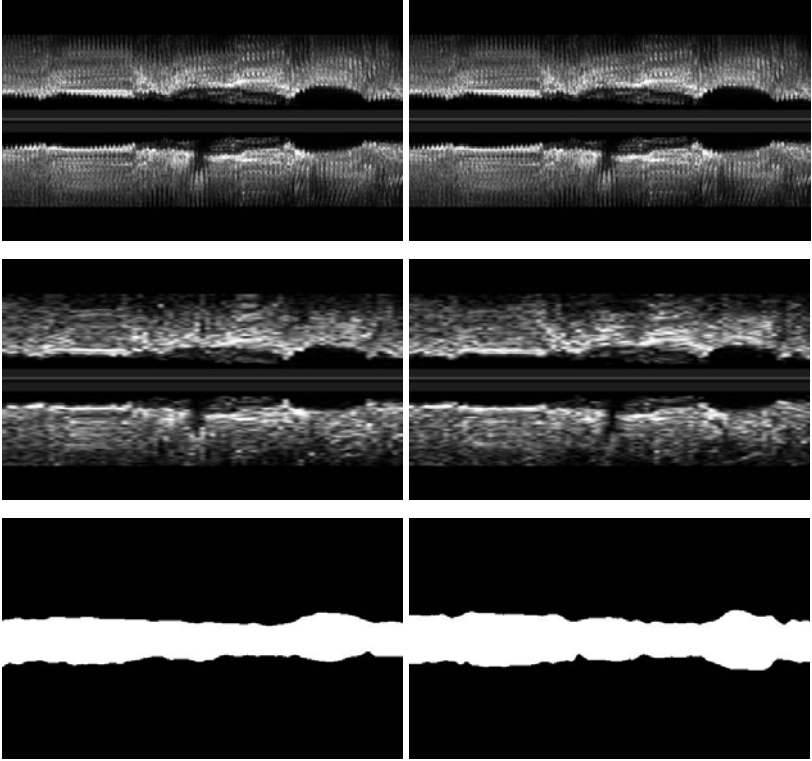
Fig. 5. *First row:* Nongated pullback. *Middle Row; Left:* Image-based gated pullback. *Right:* Ecg gated pullback. *Bottom Row; Left:* Lumen Area of image based gated pullback. *Right:* Lumen Area of ecg gated pullback.

6 Conclusion

We presented a novel image-based gating method for IVUS sequences. Our method is based on manifold learning, which embeds the similar IVUS frames onto contiguous positions of a low-dimensional manifold lying on a high dimensional image space. Further, we classified the frames by using distances between consecutive eigenvectors that represent the IVUS frames using the frame rate of the pullback and basic heart beat rate knowledge. We tested our data on 3 patients and 6 in-vivo pullbacks. We compared the number of selected frames and the lumen areas in 4 different longitudinal views, computed by both methods. Future directions for this work include analysis of lumen volume differences and the plaque areas of the gated pullbacks.

References

1. Bruining, N., von Birgelen, C., de Feyter, P.J., Ligthart, J., Li, W., Serruys, P.W., Roelandt, J.: Ecg-gated versus nongated three-dimensional intracoronary ultrasound analysis: Implications for volumetric measurements. Catheterization and Cardiovascular Diagnosis 43, 254–260 (1998)
2. Arbab-Zadeh, A., DeMaria, A.N., Penny, W., Russo, R., Kimura, B., Bhargava, V.: Axial movement of the intravascular ultrasound probe during the cardiac cycle: Implications for three-dimensional reconstruction and measurements of coronary dimensions. American Heart Journal 138, 865–872 (1999)
3. de Winter, S.A., Hamers, R., Degertekin, M., Tanabe, K., Lemos, P.A., Serruys, P.W., Roelandt, J.R.T.C., Bruining, N.: A novel retrospective gating method for intracoronary ultrasound images based on image properties. Computers in Cardiology, 13–16 (2003)
4. Zhu, H., Oakeson, K.D., Friedman, M.H.: Retrieval of cardiac phase from IVUS sequences. In: Medical Imaging 2003: Ultrasonic Imaging and Signal Processing, vol. 5035, pp. 135–146 (2003)
5. O'Malley, S.M., Carlier, S.G., Naghavi, M., Kakadiaris, I.A.: Image-based frame gating of IVUS pullbacks: A surrogate for ecg. In: Proc. IEEE International Conference on Acoustics, Speech and Signal Processing ICASSP 2007, April 15-20, vol. 1, pp. I-433–I-436 (2007)
6. O'Malley, S.M., Carlier, S.G., Naghavi, M., Kakadiaris, I.A.: Image-based frame gating for contrast-enhanced IVUS sequences. In: Proceedings of Computer Vision for Intravascular and Intracardiac Imaging (CVII), Copenhagen, Denmark (October 2006)
7. Gatta, C., Pujol, O., Leor, O.R., Ferre, J.M., Radeva, P.: Robust image-based ivus pullbacks gating. Med. Image. Comput. Assist. Interv. Int. 11(Pt 2), 518–525 (2008)
8. Schumacher, A.: Linear and Nonlinear Approaches to the Analysis of R-R Interval Variability. Biological Research For Nursing 5(3), 211–221 (2004)
9. Malpas, S.C.: Neural influences on cardiovascular variability: possibilities and pitfalls. Am. J. Physiol. Heart. Circ. Physiol. 282(1), H6–H20 (2002)
10. Tenenbaum, J.B., Silva, V., Langford, J.C.: A global geometric framework for nonlinear dimensionality reduction. Science 290(5500), 2319 (2000)
11. Roweis, S.T., Saul, L.K.: Nonlinear Dimensionality Reduction by Locally Linear Embedding. Science 290(5500), 2323–2326 (2000)
12. Belkin, M., Niyogi, P.: Laplacian eigenmaps for dimensionality reduction and data representation. Neural Comput. 15(6) (2003)